Supplement to: Maass PG, Aydin A, Luft FC, et al.,

***PDE3A* mutations in autosomal-dominant hypertension with brachydactyly**

The authors provide this appendix to give readers additional information about their work.

Supplementary Methods

Table S1. Clinical phenotypes of all investigated families.

	Turkey	France	USA	South Africa	Canada I	Canada II
patients	30	3	3	1	6	4
***PDE3A* mutation**	T445N	T445A	T445S	A447T	G449V	A447V
hypertension	yes	yes	yes	yes	yes	yes
Severe BDE	yes [except VI/9]	yes	yes	yes	yes	yes
Short stature	yes	yes	yes	yes	yes	yes
PICA loops	yes	NA	yes	NA	NA	NA

Bilginturan and colleagues described autosomal-dominant hypertension with type E brachydactyly (BDE) in 1973.[1] We mapped the syndrome with linkage to chromosome 12p, determined that by age 50 affected persons had a 50 mm Hg increase in mean arterial blood pressure, compared to non-affected relatives, that plasma renin activity, aldosterone, and norepinephrine responded to volume expansion and contraction normally, and that severe heart disease or lipid disturbances were not a part of the syndrome.[2] We found that blood pressure was lowered by about 8 mm Hg with all classes of hypertensive drugs, that neurovascular contact between the posterior-inferior cerebellar artery existed, and that baroreflex regulation differed in affected and non-affected persons.[3,4] We found that affected persons did not conduct normal buffering of blood pressure,[5] despite normal appearing muscle sympathetic nerve activity and physiologically inspected candidate genes.[6] We observed that milrinone and diazoxide did not differ in terms of affecting forearm blood flow than placebo and determined the presence of chromosomal inversions, deletions, and reinsertions within the linkage interval.[7] Subsequently, we confirmed the linkage interval with a SNP analysis and found that the blood pressure phenotype is detectable in childhood even before the BDE phenotype.[8] The BDE phenotype typically includes thickening and shortening of metacarpal and phalangeal bones. Interfamilial differences concerning the severity, the affected bones, and the appearance of cone-shaped epiphysis can occur.[9] The severity of the phenotypes was confirmed in several studies. Additional families were phenotyped by collaborators and their DNA samples referred to us.[10] The family trees are shown in Figure 1. NA = no data available

Figure S1. PDE3A conservation and whole-genome sequencing.

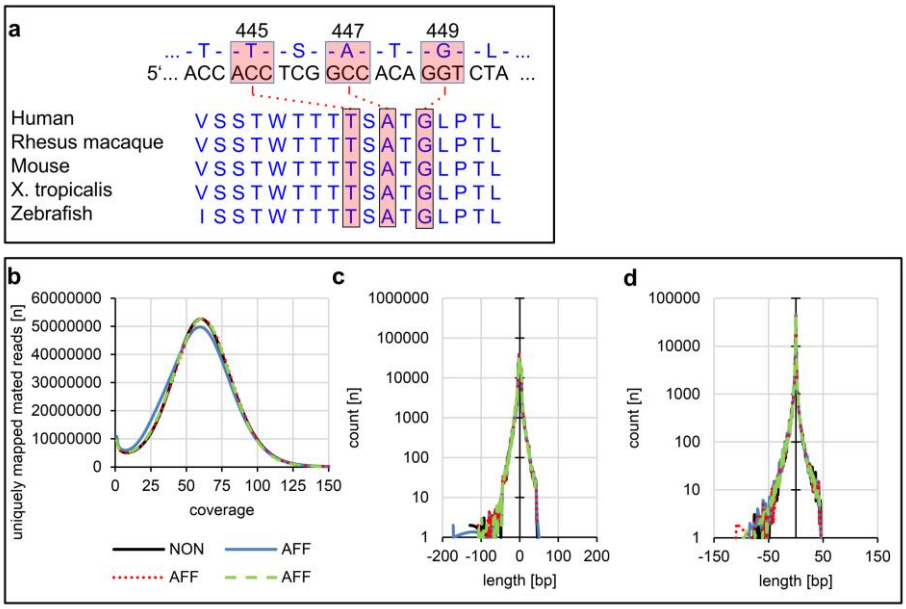

(a) Multiple sequence alignment of the PDE3A peptide sequence near the identified mutations in five different species. The mutations were in a highly conserved PDE3A domain. **(b)** Genomic coverage of Complete Genomics' (CG) whole genome sequencing of Turkish family members IV/6, IV/7, V/14, V/30. A mean coverage of 57.39±0.25x for each of the four samples was reached. **(c)** The detected insertion and deletion (indels) events compared to the genome assembly hg19. **(d)** The substitution events are summarized. To use the complementary advantage of different genome sequencing platforms, we performed whole-genome sequencing of the same Turkish patient whose DNA was also sequenced by CG, on the Illumina platform to screen for further small sequence variations, structural variants and the inversion breakpoints, that were found in fibroblasts and LCL by interphase FISH.[11] Among the more than three million SNV and small indels, we identified the missense mutation in *PDE3A* that has also been detected in CG sequencing. NM_000921:exon4:c.1334C>A:p.T445N affects a highly conserved amino acid and was not observed in the 1000-genomes data nor in the 5000-exomes data (Exome Variant Server, http://evs.gs.washington.edu/EVS/ [July 2013 accessed]), in Sanger sequencing of all non-affected family members, or in 200 unrelated Caucasian controls.[12]

Table S2. Re-sequenced variations within the Turkish linkage region.

no.	DNA	locus	ploidy	allele	chr12	begin	end	varType	reference	alleleseq	total score
1	AFF1	11148630	2	1	chr12	17888502	17888502	ins		GGA	119
	AFF2	11182511	2	1	chr12	17888502	17888502	ins		GGA	129
	AFF3	11269475	2	1	chr12	17888502	17888502	ins		GGA	75
2	AFF1	11151178	2	1	chr12	18243531	18243531	ins		A	93
	AFF2	11185097	2	1	chr12	18243531	18243531	ins		A	87
	AFF3	11271977	2	1	chr12	18243531	18243531	ins		A	125
3	AFF1	11151370	2	1	chr12	18254519	18254521	del	GT		184
	AFF2	11185273	2	1	chr12	18254519	18254521	del	GT		375
	AFF3	11272149	2	1	chr12	18254519	18254521	del	GT		253
4	AFF1	11153010	2	1	chr12	18675785	18675797	del	TTAGGAACTCCT		124
	AFF2	11186763	2	1	chr12	18675785	18675797	del	TTAGGAACTCCT		224
	AFF3	11273875	2	1	chr12	18675785	18675797	del	TTAGGAACTCCT		274
5	AFF1	11153492	2	1	chr12	18801113	18801117	del	GTTT		41
	AFF2	11187207	2	1	chr12	18801113	18801117	del	GTTT		54
	AFF3	11274287	2	1	chr12	18801113	18801117	del	GTTT		59
6	AFF1	11156136	2	1	chr12	19323219	19323219	ins		A	68
	AFF2	11189859	2	1	chr12	19323219	19323219	ins		A	63
	AFF3	11276865	2	1	chr12	19323219	19323219	ins		A	66
7	AFF1	11157160	2	1	chr12	19503703	19503703	ins		A	70
	AFF2	11190833	2	1	chr12	19503703	19503703	ins		A	113
	AFF3	11277903	2	1	chr12	19503703	19503703	ins		A	104
8	AFF1	11159920	2	1	chr12	19911863	19911863	ins		A	167
	AFF2	11193781	2	1	chr12	19911863	19911863	ins		A	124
	AFF3	11280953	2	1	chr12	19911863	19911863	ins		A	122
9	AFF1	11161094	2	1	chr12	20071553	20071553	ins		A	149
	AFF2	11195109	2	1	chr12	20071553	20071553	ins		A	125
	AFF3	11282039	2	1	chr12	20071553	20071553	ins		A	119
10	AFF1	11162980	2	1	chr12	20414800	20414802	del	TT		319
	AFF2	11196967	2	1	chr12	20414800	20414802	del	TT		235
	AFF3	11283997	2	1	chr12	20414800	20414802	del	TT		222
11	AFFall	11163748	2	1	chr12	20610019	20610027	del	CAAACAAA		130
12	AFFall	11384487	2	1	chr12	20767932	20767937	del	TCTTT		120
13	AFFall	11166688	2	1	chr12	20993338	20993343	del	TTTTT		69
14	AFFall	11166764	2	1	chr12	20998242	20998256	sub	CAATGAGT AGAAAC	ACCT TTTG TTTG	59
15	AFFall	11166796	2	1	chr12	21000481	21000483	del	AT		316
16	AFFall	11167664	2	1	chr12	21079950	21079955	del	GAGTT		85
17	AFFall	11387681	2	1	chr12	21113967	21113969	del	AA		120
18	AFF1	11170944	2	1	chr12	21470951	21470951	ins		A	103
	AFF2	11204447	2	1	chr12	21470951	21470951	ins		A	105
	AFF3	11291919	2	1	chr12	21470951	21470951	ins		A	24
	AFF3	11291919	2	2	chr12	21470951	21470951	ins		A	121
19	AFF1	11172020	2	1	chr12	21595552	21595556	del	GGAA		528

	AFF2	11205649	2	1	chr12	21595552	21595556	del	GGAA		327
	AFF3	11293127	2	1	chr12	21595552	21595556	del	GGAA		281
20	AFF1	11172488	2	1	chr12	21668265	21668266	del	T		75
	AFF2	11206337	2	1	chr12	21668265	21668266	del	T		130
	AFF3	11293797	2	1	chr12	21668265	21668266	del	T		127
21	AFF1	11173014	2	1	chr12	21737302	21737339	sub	TGTGAGTGCTCACCAATGGGTGACCTCAGCAGAAGAG	CTT	121
	AFF2	11206843	2	1	chr12	21737302	21737339	sub	TGTGAGTGCTCACCAATGGGTGACCTCAGCAGAAGAG	CTT	128
	AFF3	11294321	2	1	chr12	21737302	21737339	sub	TGTGAGTGCTCACCAATGGGTGACCTCAGCAGAAGAG	CTT	77
	AFF2	11206843	2	2	chr12	21737302	21737339	sub	TGTGAGTGCTCACCAATGGGTGACCTCAGCAGAAGAG	CTT	128
	AFF3	11294321	2	2	chr12	21737302	21737339	sub	TGTGAGTGCTCACCAATGGGTGACCTCAGCAGAAGAG	CTT	123
22	AFFall	11173410	2	1	chr12	21781705	21781709	del	ATTA		42
23	AFFall	11173610	2	1	chr12	21800722	21800731	sub	CGGGTTCAA	TGT	115
24	AFF1	11173846	2	1	chr12	21845628	21845628	no-call		?	
	AFF2	11207677	2	1	chr12	21845628	21845628	no-call		?	
	AFF3	11295135	2	1	chr12	21845628	21845628	no-call		?	
25	AFF1	11173916	2	1	chr12	21890351	21890355	del	TTTG		281
	AFF2	11207783	2	1	chr12	21890351	21890355	del	TTTG		376
	AFF3	11295221	2	1	chr12	21890351	21890355	del	TTTG		125
	AFF3	11295221	2	2	chr12	21890351	21890355	del	TTTG		125
26	AFFall	11393913	2	1	chr12	22109144	22109159	del	TTTTTTTTTTTTTTT		41
27	AFF1	11175622	2	1	chr12	22226277	22226277	ins		A	61
	AFF2	11209579	2	1	chr12	22226277	22226277	ins		A	62
	AFF3	11296973	2	1	chr12	22226277	22226277	ins		A	48
28	AFF1	11177094	2	1	chr12	22447228	22447229	del	T		124
	AFF2	11211011	2	1	chr12	22447228	22447229	del	T		128
	AFF3	11298615	2	1	chr12	22447228	22447229	del	T		59
29	AFF1	11177120	2	1	chr12	22455169	22455169	ins		CTT	71
	AFF2	11211049	2	1	chr12	22455169	22455169	ins		CTT	204
	AFF3	11298647	2	1	chr12	22455169	22455169	ins		CTT	181
30	AFF1	11177190	2	1	chr12	22469859	22469859	ins		A	78
	AFF2	11211133	2	1	chr12	22469859	22469859	ins		A	62
	AFF3	11298721	2	1	chr12	22469859	22469859	ins		A	127
31	AFF1	11178446	2	1	chr12	22750090	22750090	ins		A	75
	AFF2	11212547	2	1	chr12	22750090	22750090	ins		A	110
	AFF3	11300149	2	1	chr12	22750090	22750090	ins		A	26
	AFF3	11300149	2	2	chr12	22750090	22750090	ins		A	121
32	AFFall	11398949	2	1	chr12	22867838	22867840	del	TC		120

33	AFFall	11399621	2	1	chr12	23011554	23011573	del	TACTATTTCTTGCACTGGG		80
34	AFF1	11179842	2	1	chr12	23060480	23060483	del	GGG		87
	AFF2	11213973	2	1	chr12	23060480	23060483	del	GGG		283
	AFF3	11301537	2	1	chr12	23060480	23060483	del	GGG		305
35	AFFall	11400153	2	1	chr12	23166252	23166255	del	CAA		410
36	AFF1	11181664	2	1	chr12	23403279	23403279	no-call		?	
	AFF2	11215843	2	1	chr12	23403279	23403279	no-call		?	
	AFF3	11303229	2	1	chr12	23403279	23403279	no-call		?	
37	AFFall	11182206	2	1	chr12	23518569	23518573	del	TAAG		162
38	AFF1	11182984	2	1	chr12	23649317	23649322	no-call	TTTTT	?	
	AFF2	11217161	2	1	chr12	23649317	23649322	no-call	TTTTT	?	
	AFF3	11304539	2	1	chr12	23649317	23649322	no-call	TTTTT	?	
39	AFF1	11183584	2	1	chr12	23744020	23744025	del	TTTAT		53
	AFF2	11217755	2	1	chr12	23744020	23744025	del	TTTAT		390
	AFF3	11305201	2	1	chr12	23744020	23744025	del	TTTAT		258
40	AFF1	11183854	2	1	chr12	23791793	23791793	ins		A	146
	AFF2	11218065	2	1	chr12	23791793	23791793	ins		A	120
	AFF3	11305503	2	1	chr12	23791793	23791793	ins		A	126

Figure S2. MRI of VI/9.

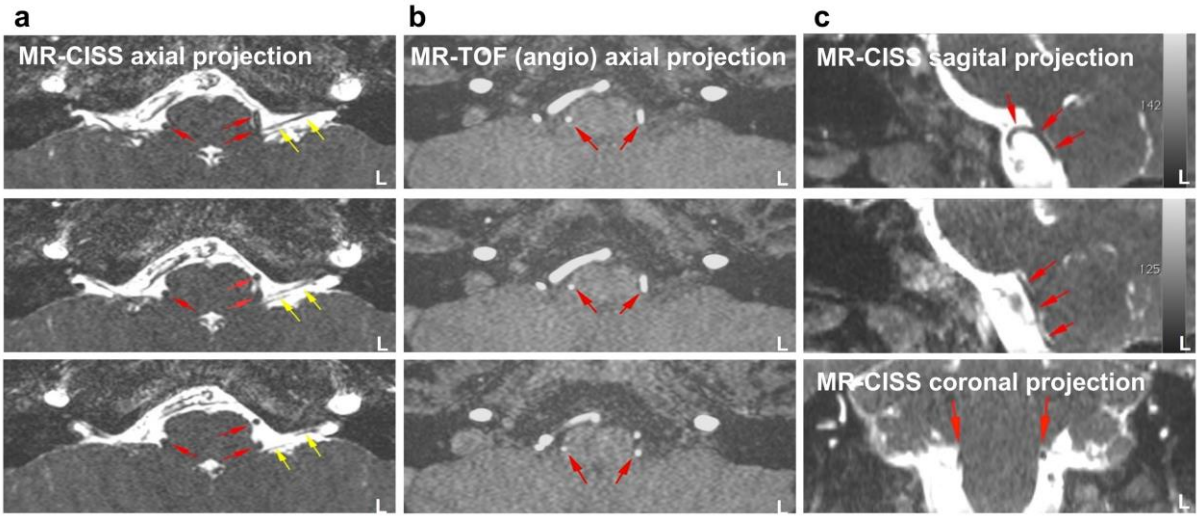

(a) MRI of the hypertensive teenager with mild BDE (VI/9). The red arrows indicate the contacting vessels to the ventrolateral medulla (VLM) on the left and right side. On the left side, the PICA is the offending artery indicating a type 1 neurovascular contact (nvc). The yellow arrows indicate the cranial nerves IX & X. **(b)** The red arrows indicate the contacting vessels to the VLM. **(c)** The upper picture shows the left VLM. The red arrows indicate the PICA as an impressive loop contacting the VLM as type 1 nvc. The arrows in the middle picture document the PICA attached to the right VLM. The coronal projection displays the vessel signal on both sides of the VLM.

Figure S3. *Pde3a in situ* hybridization and characterization of human chondrogenically-induced fibroblasts.

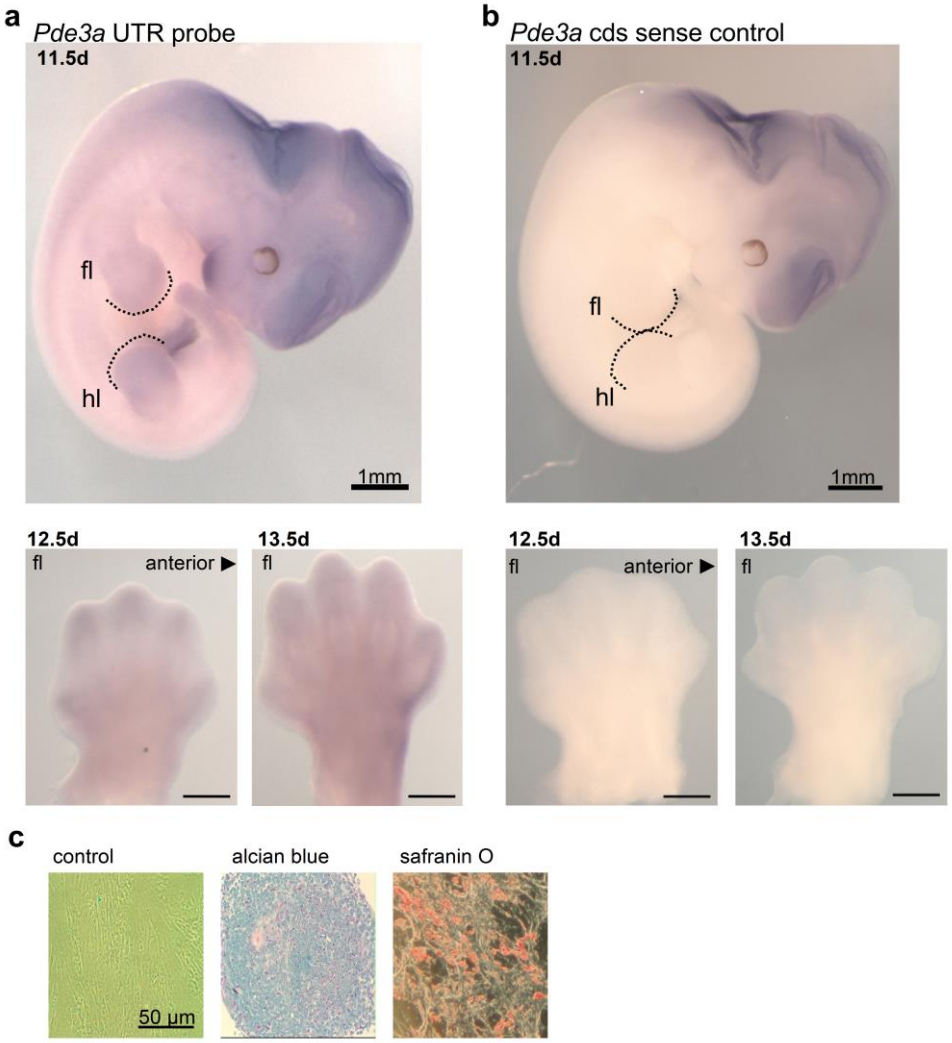

(a) Murine *in situ* hybridization with 3' UTR probe in *Pde3a* detected light limb bud expression in embryos of 12.5 and 13.5d. **(b)** The *in situ* antisense control probe in the coding sequence of *Pde3a* (cds) showed no expression in the developing limb buds. **(c)** Successful chondrogenic induction of human fibroblasts from buttock biopsies after 3 weeks in pellet culture. We used chondrogenically induced fibroblasts to focus on the chondrogenic *PTHLH* expression. Since we were able to obtain more fibroblasts from non-affected and related controls than MSC from the Turkish family, we performed *PTHLH* expression experiments on chondrogenically induced fibroblasts. After embedding and sectioning, alcian blue or safranin O stainings detected extra cellular matrix proteins that are characteristic for cartilage.

Figure S4. cAMP and cGMP quantifications, and Lineweaver-Burke plots of Michaelis-Menten kinetics

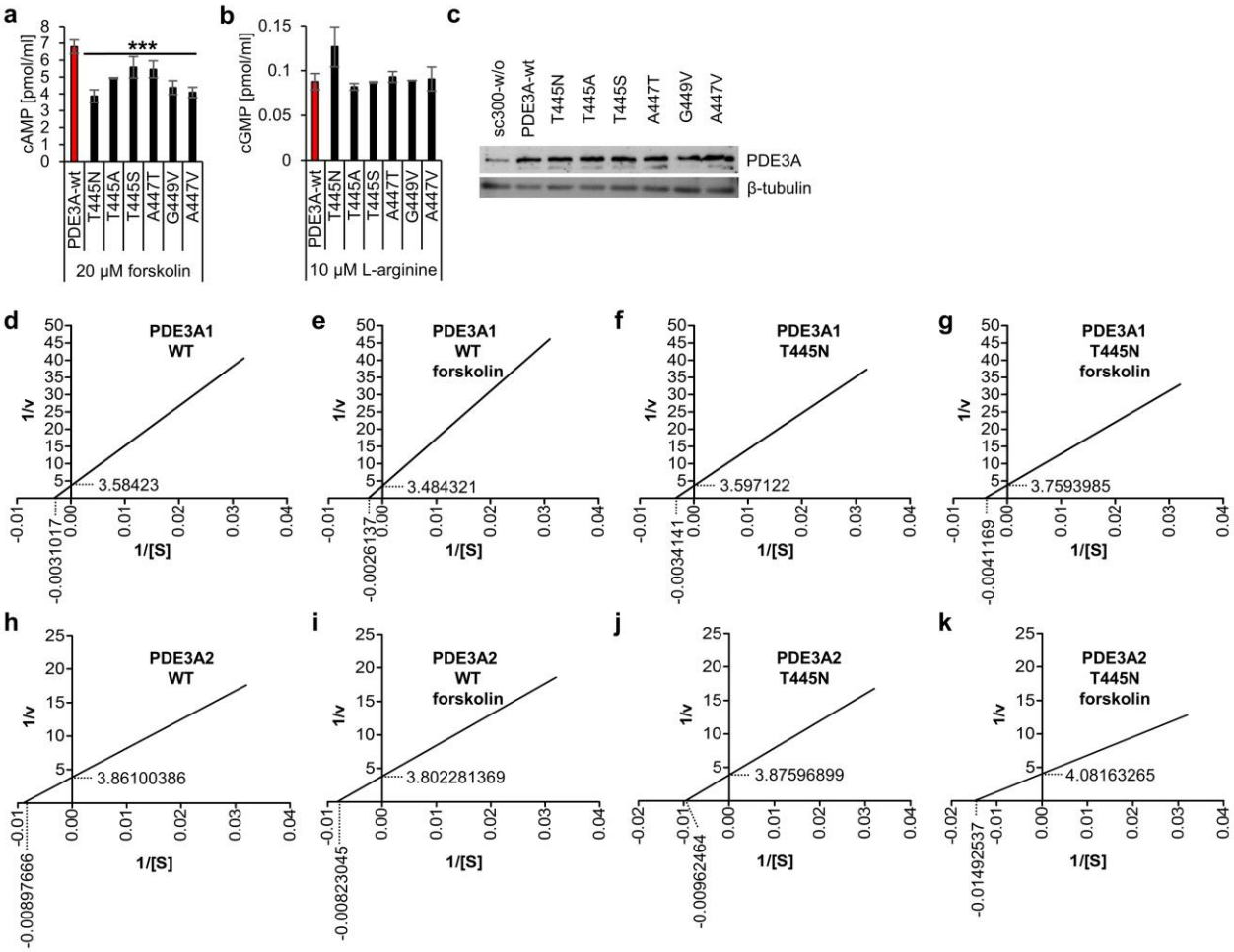

HeLa cells were transiently transfected with the full-length wildtype *PDE3A* construct and the six full-length *PDE3A* mutations; forskolin or L-arginine stimulation was performed to enhance intracellular cAMP or cGMP levels through adenylate or guanylate cyclase activation. 48 h after transfection, cells were harvested to determine cAMP **(a)** and cGMP **(b)** levels in enzyme immuno-assays. The data shown are results of three independent experiments with minimum and maximum deviation. Significant differences were determined between PDE3A-wildtype (wt) and the mutations, defining the mutations as gain-of-function mutations, causing increased cAMP hydrolysis (n = 4, two-tailed Student's T-test). cGMP levels were not altered in the presence of the PDE3A mutations (n = 6). **(c)** Western blotting detected the successful expression of wildtype and the PDE3A mutant proteins, transfected as

expression constructs in HeLa cells. Controls were empty vector transfected cells. **(d-g)** Linear regression analysis of transformed Michaelis-Menten data from Figure 3a of FLAG-tagged PDE3A1 WT, PDE3A1 T445N, and **(h-k)** linear regression analysis of transformed Michaelis-Menten data from Figure 3b of FLAG tagged PDE3A2 WT and PDE3A2 T445N, visualized as Lineweaver-Burke plots.

Figure S5. IC_{50} measurement of cGMP

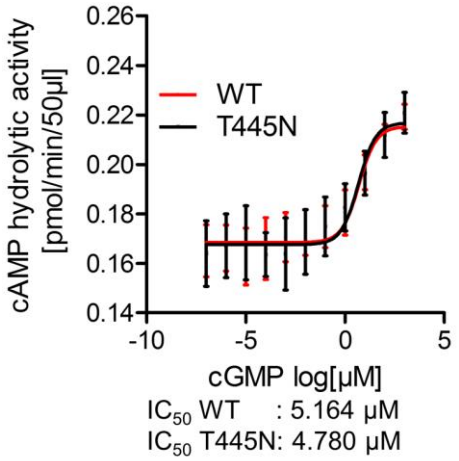

cGMP competitively inhibits PDE3A, but equivalent values were determined for FLAG-tagged PDE3A1 wildtype (WT) and the tagged PDE3A1 T445N mutant. IC_{50} for WT was 5.164 µM; 4.78 µM for T445N (n = 3). Relevant differences were not determined in three independent experiments.

Figure S6. Functional CRE-luciferase assays in HeLa cells transiently expressing the six PDE3A mutations.

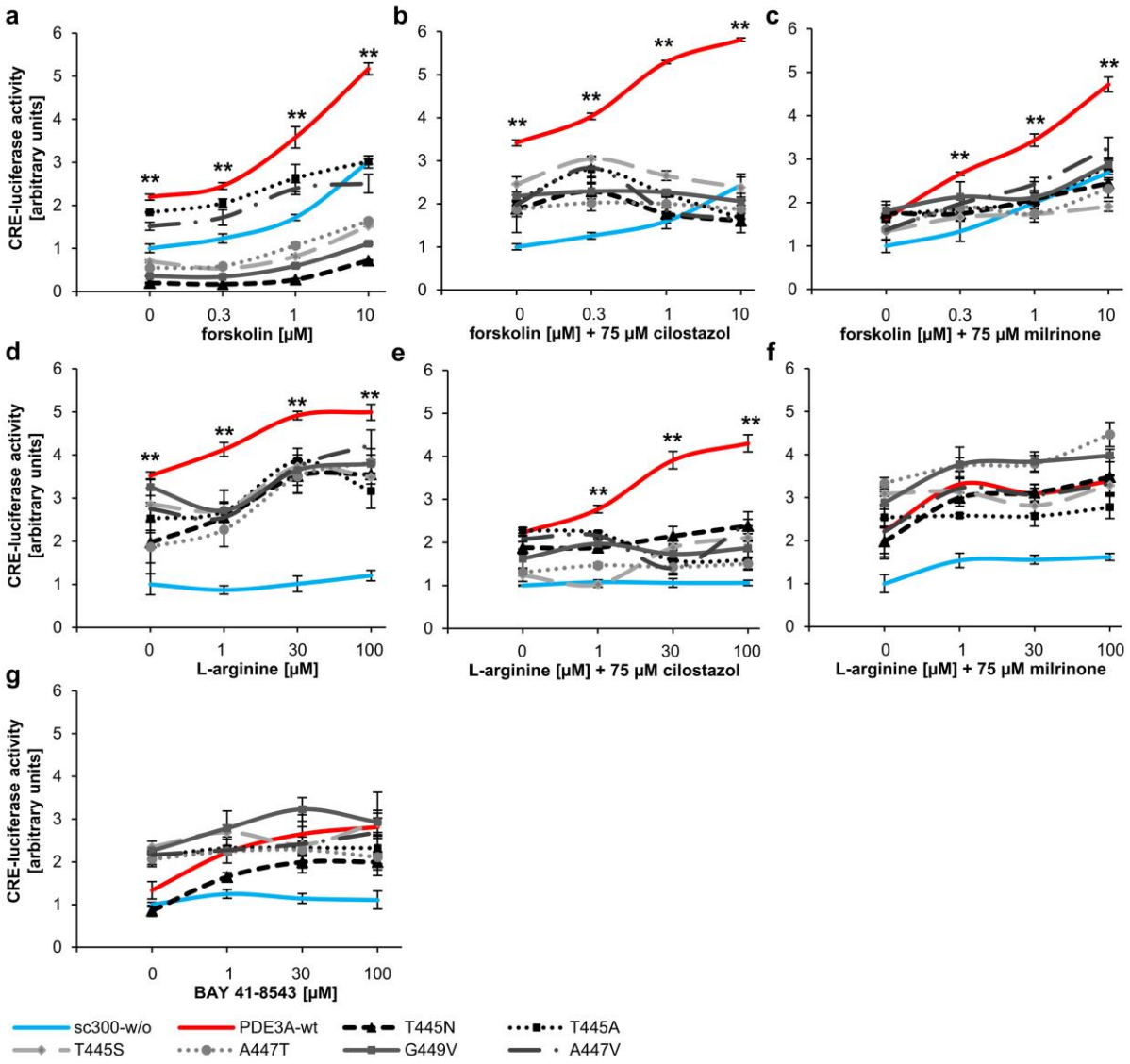

(a) HeLa cells were transfected with an empty vector (sc300-w/o, blue line), a full-length wildtype *PDE3A* expression construct (red line), and the six full-length *PDE3A* mutations' expression plasmids (grey and black lines). HeLa cells were co-transfected with a cAMP responsive element (CRE) regulating luciferase transcriptional activity under the influence of increasing forskolin concentrations to further elucidate the functional consequences of the PDE3A mutations ($p<0.002$). A renilla luciferase vector was used for standardization. The data describe the relative increase of luciferase activity normalized to the DMSO control of empty-vector transfected cells. The results are means of three independent transfections

(mean±SD; n = 3; Wilcoxon-Mann-Whitney test). The more hydrolyzed cAMP, the less luciferase expression. In the presence of incremental forskolin concentrations enhancing cAMP levels, the *PDE3A* mutations showed a significant reduction of the CRE-mediated luciferase activity as a result of the higher cAMP hydrolysis compared to the wildtype PDE3A. **(b)** The mutated PDE3A proteins hydrolyzed more cAMP in the presence of cilostazol, compared to controls ($p<0.002$). **(c)** Milrinone decreased the enhanced cAMP hydrolysis more effectively than cilostazol with increasing cAMP levels ($p<0.002$). The effect on the mutants was less than on wildtype PDE3A cAMP hydrolysis. **(d)** cGMP stimulation with increasing L-arginine concentrations, with and without cilostazol or milrinone, showed that cGMP competitively inhibited cAMP hydrolysis with a significant difference between mutants and wildtype PDE3A ($p<0.002$). The more cGMP present, the less cAMP hydrolysis, and the greater the luciferase activity. **(e)** Cilostazol abrogated the inhibitory effect of the increasing L-arginine concentrations on the mutants more than the wildtype PDE3A ($p<0.002$). **(f)** cGMP inhibition and milrinone were synergistic and equalized the mutants' and the wildtype PDE3A hydrolytic activities. **(g)** The soluble guanylate cyclase (sGC) stimulator BAY 41-8543 reduced the enhanced cAMP hydrolysis of the *PDE3A* mutations compared to the wildtype PDE3A. A statistical significance between the luciferase activities of the *PDE3A* mutations *versus* the wildtype PDE3A in the panels f and g was not reached.

Figure S7. Characterization of MSC and MSC-derived cells.

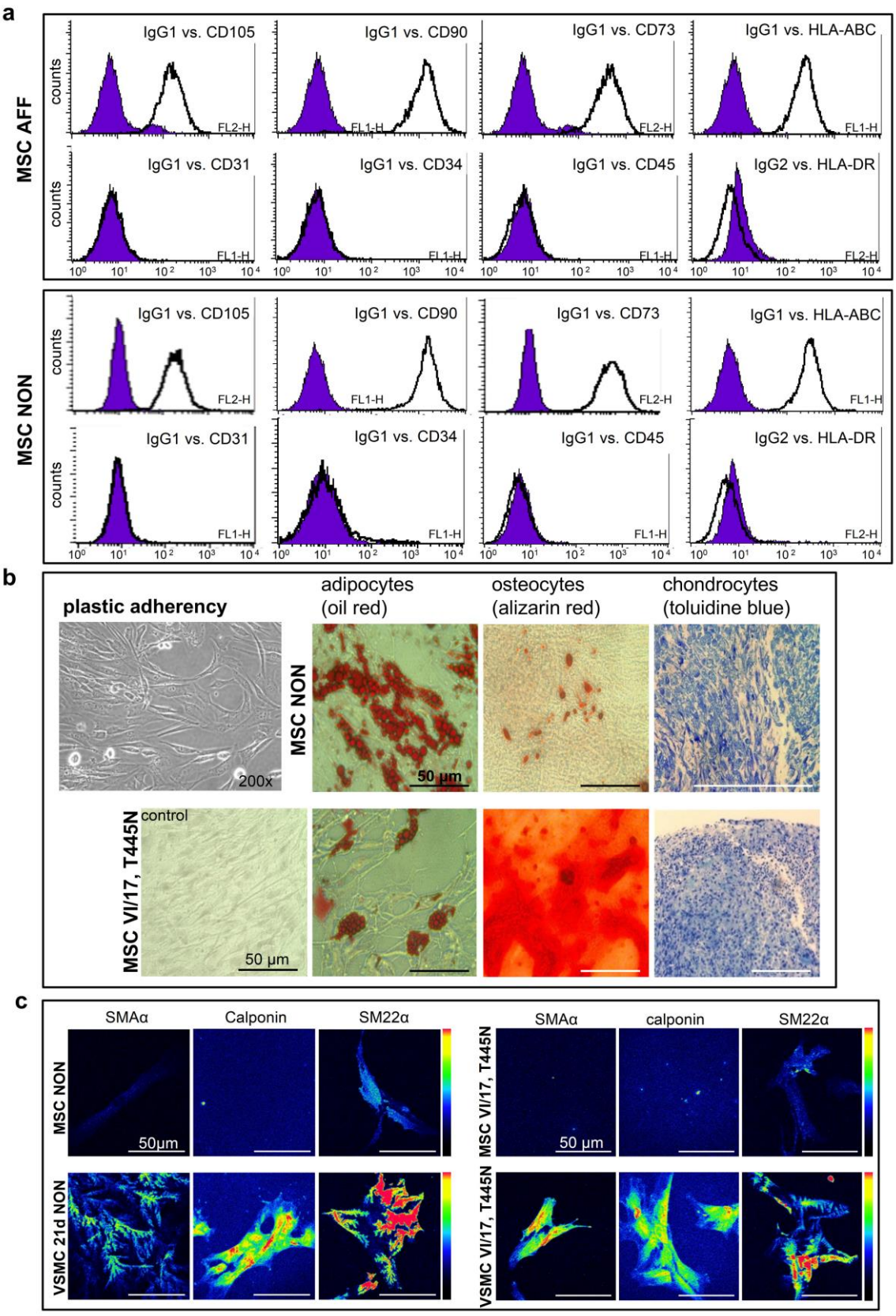

(a) FACS results of the affected patient VI/17 and one non-affected control. The analysis of surface markers detected $CD105^{+}$, $CD90^{+}$, $CD73^{+}$, HLA-ABC^{+}, $CD31^{-}$, $CD34^{-}$, $CD45^{-}$ and HLA-DR^{-} cells. **(b)** Plastic adherence and the multilineage potential of MSCs of one non-affected control and VI/17. MSC and VSMC of patient VI/9 and the second non-affected control were identically characterized and fulfilled all criteria of MSC and VSMC (data not shown). Immuno-cytochemical stainings of the MSC-derived adipocytes, osteocytes, and chondrocytes validated the multilineage potential. The fatty vacuoles determined the successful differentiation into adipocytes; calcium precipitates characterized MSC-derived osteocytes. Toluidine blue stained proteoglycans of sectioned chondrogenic tissue that was generated in micro-mass pellet cultures. The successful differentiation was similar in the MSCs of the controls and the affected patient VI/17. The MSC characterizations fulfilled the criteria of the International Society for Cellular Therapy.[13] **(c)** Myogenic differentiation of one non-affected control and MSCs of VI/17 into vascular smooth muscle cells (VSMC) after 21 days of differentiation. Semi-quantitative immunofluorescence detected the smooth muscle markers smooth muscle actin (SMAα), calponin and transgelin (SM22α) that were highly expressed compared to undifferentiated mesenchymal stromal cells (MSC).[14] The color spectrum indicates the expression level from low (black) to high (red).

Figure S8. PDE3A overexpression in HeLa cells and carboxyfluorescein-diacetate-succinimidyl-ester (CFSE) signal quantification in FACS analysis.

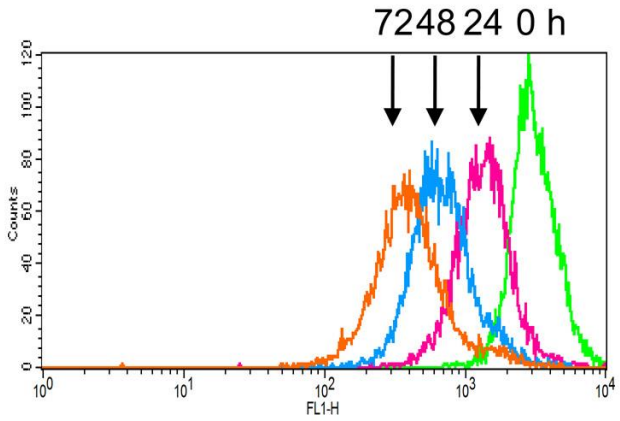

Intensity histogram of flow cytometry analysis of CFSE-labeled and transfected HeLa cells. After CFSE labeling, the cells were seeded and transfected with full-length wildtype *PDE3A* or full-length *PDE3A* expressing the six mutations, the next day. Measurements were performed at 24, 48 and 72 h post transfection to determine the proliferation rates. Due to mitosis and the distribution of CFSE, the signal intensity changed in the measured time of 72 h.

Figure S9. Individual Western blotting experiments.

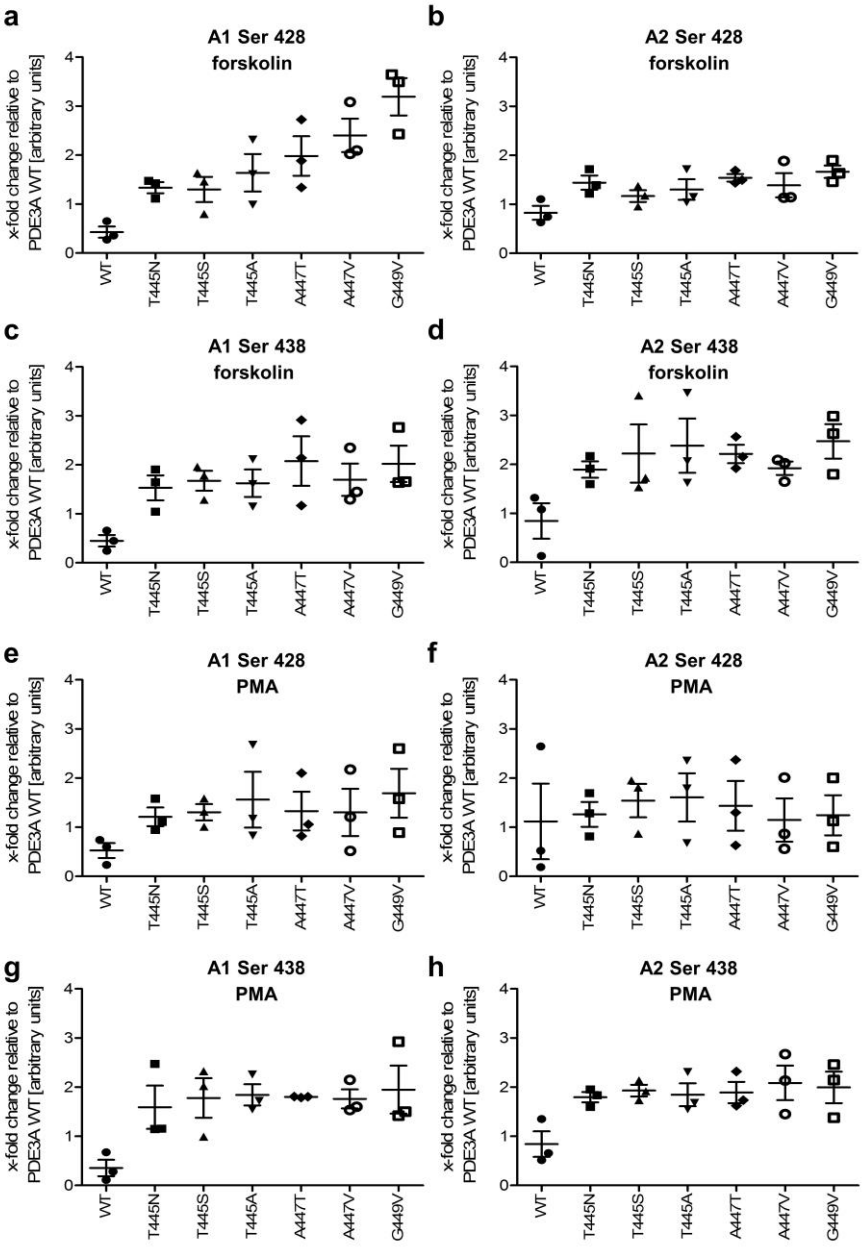

(a-h) Individual quantification of Western blot signals of each PDE3A mutation of the three independent experiments shown in Figure 4a and 4b. The signals were densitometrically quantified in relation to the loading control β-tubulin. Due to experimental variation and quality differences of the anti-phospo antibodies, differences of the investigated phosphorylations of Ser^{428} and Ser^{438} in PDE3A1 and PDE3A2 occurred. However, the pooled results (Figure 4a, b) of all mutations showed statistical significance compared to PDE3A wildtype (WT) in non-parametrical Mann-Whitney rank sum testing.

Figure S10. PKA and PKC phosphorylate PDE3A Ser^{438}.

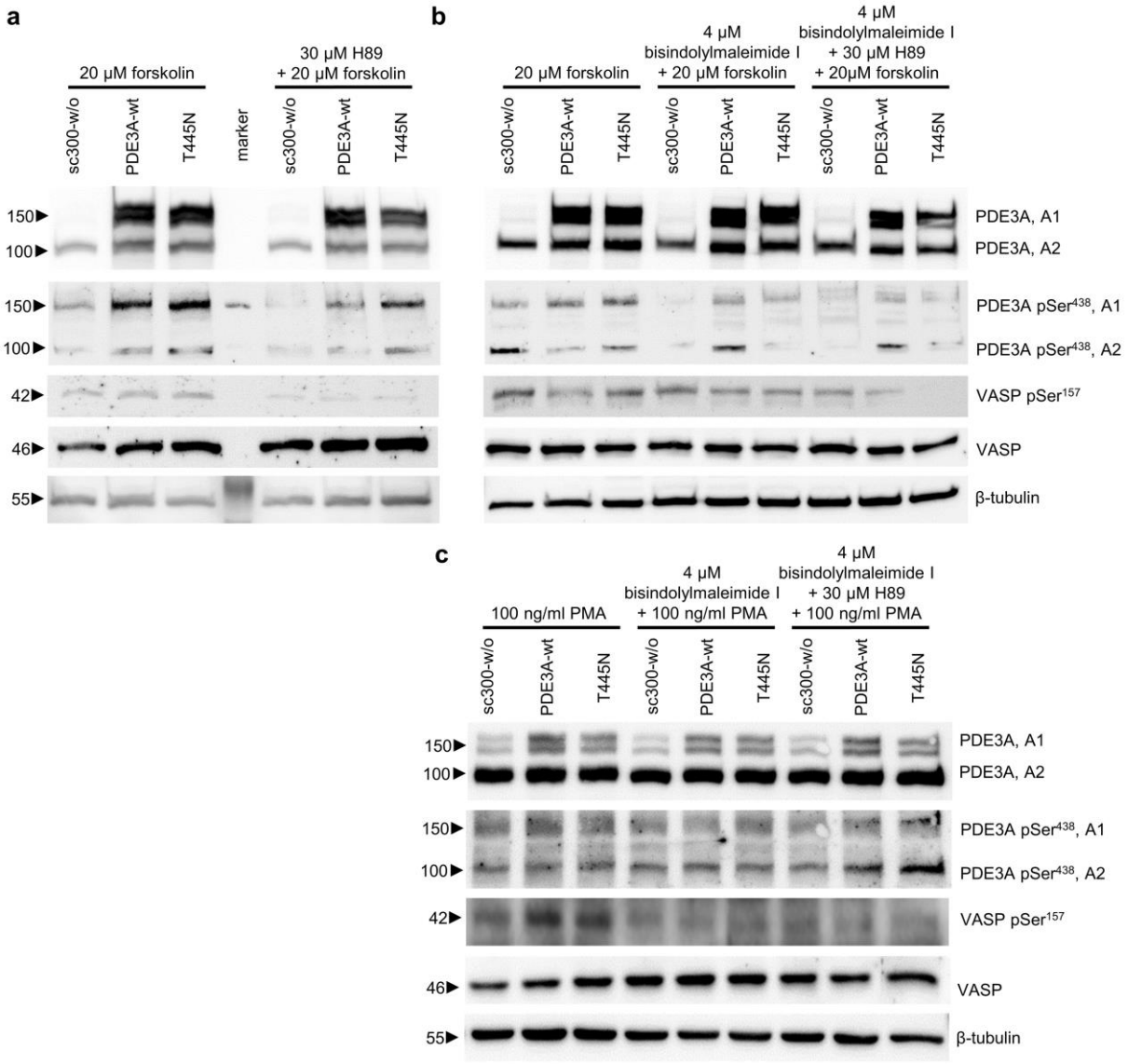

(a) Full-length wildtype (NM_000921) and T445N PDE3A were transiently expressed in HeLa cells. In forskolin-stimulated cells, the T445N PDE3A Ser^{438} phosphorylation was increased compared to wildtype (WT) and mock control (sc300 w/o). The use of the PKA inhibitor H89 revealed less Ser^{438} phosphorylation. The T445N phosphorylation was still stronger at Ser^{438} compared to controls. VASP Ser^{157} phosphorylation that is mediated by PKA was reduced in H89 PKA-inhibited cells. Non-phosphorylated VASP was not altered. **(b)** The use of PKC α, β, δ, ε and γ inhibitor bisindolylmaleimide I showed that PDE3A Ser^{438} was also phosphorylated by PKC.[15] The combination of H89 with bisindolylmaleimide I

further reduced Ser^{438} phosphorylation. Endogenous VASP was not affected. **(c)** The PMA stimulation alone and in combination with the inhibitors bisindolylmaleimide I and / or H89 showed decreased PDE3A Ser^{438} and VASP Ser^{157} phosphorylation. The detection of non-phosphorylated VASP showed no differences. However, the data suggest that further protein kinases also phosphorylate Ser^{438}. Tubulin was loading control.

Figure S11. Pyrosequencing of the *PDE3A* T445N mutation in MSC of VI/17.

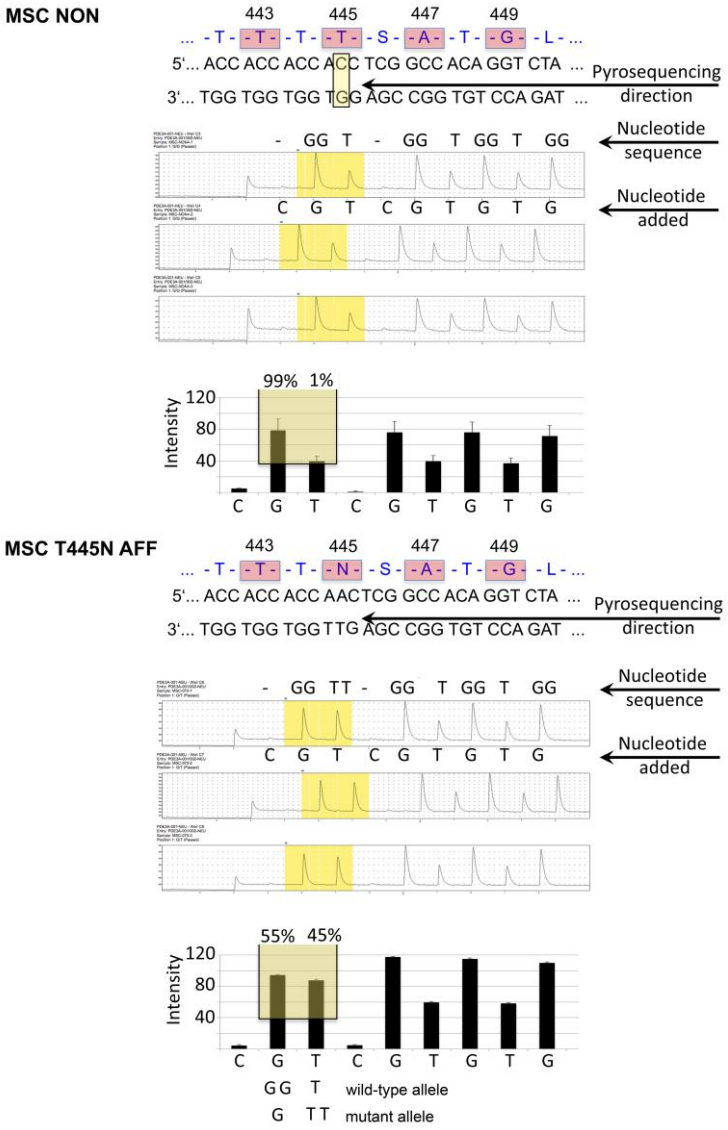

The figure shows the raw data of the *PDE3A* pyrosequencing of the T445N patient. The data shown are from a reverse pyrosequencing approach. The yellow area indicates the position of the *PDE3A* mutation. The base "G" varies between 50 and 100%, "T" varies between 0 and 50%. The data shown are from three independent replicates; error bars are SD. The presence of each allele in the reaction is displayed in percent. Compared to the wildtype allele "G" (G = 99%, T = 1%), no significant differential expression was detected for the mutated *PDE3A* allele "T" of the T445N patient (G = 55%, T = 45%). A preferred mono-allelic expression, either due to the mutation or the inversion, was excluded.

Figure S12. PDE3A, PTHrP and VASP in MSC, VSMC.

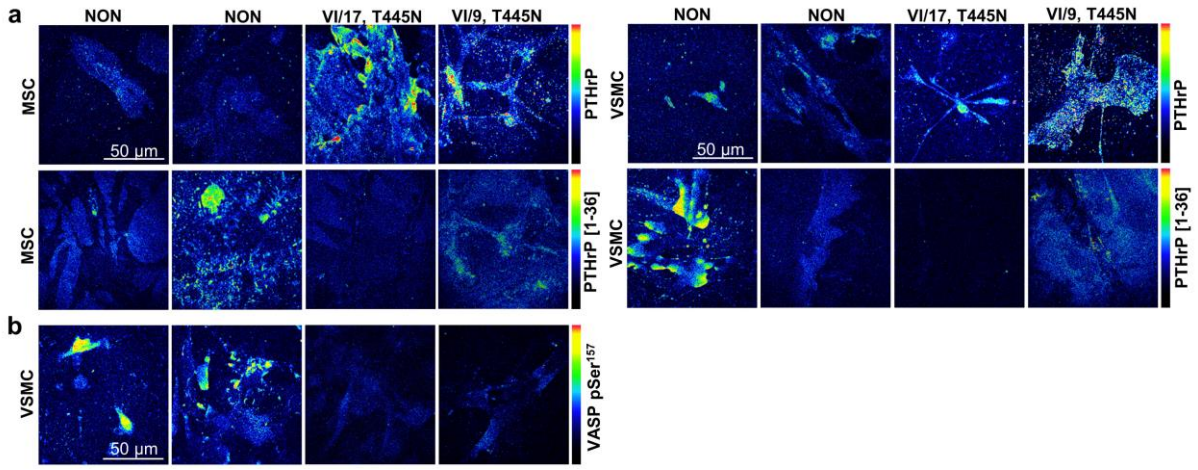

The color spectrum indicates expression levels from low (black) to high (red) in the semi-quantitative immunofluorescence. **(a)** PTHrP influences the proliferation of VSMC.[16] The PTHrP full-length protein was increased, while the PTHrP peptide was decreased in MSC and VSMC from the T445N patients. **(b)** The phosphorylation of VASP Ser^{157} was reduced in VSMC of the affected patients compared to controls; phosphorylated VASP in MSC was not detectable.

Figure S13. Peptide assays of the PDE3A mutations.

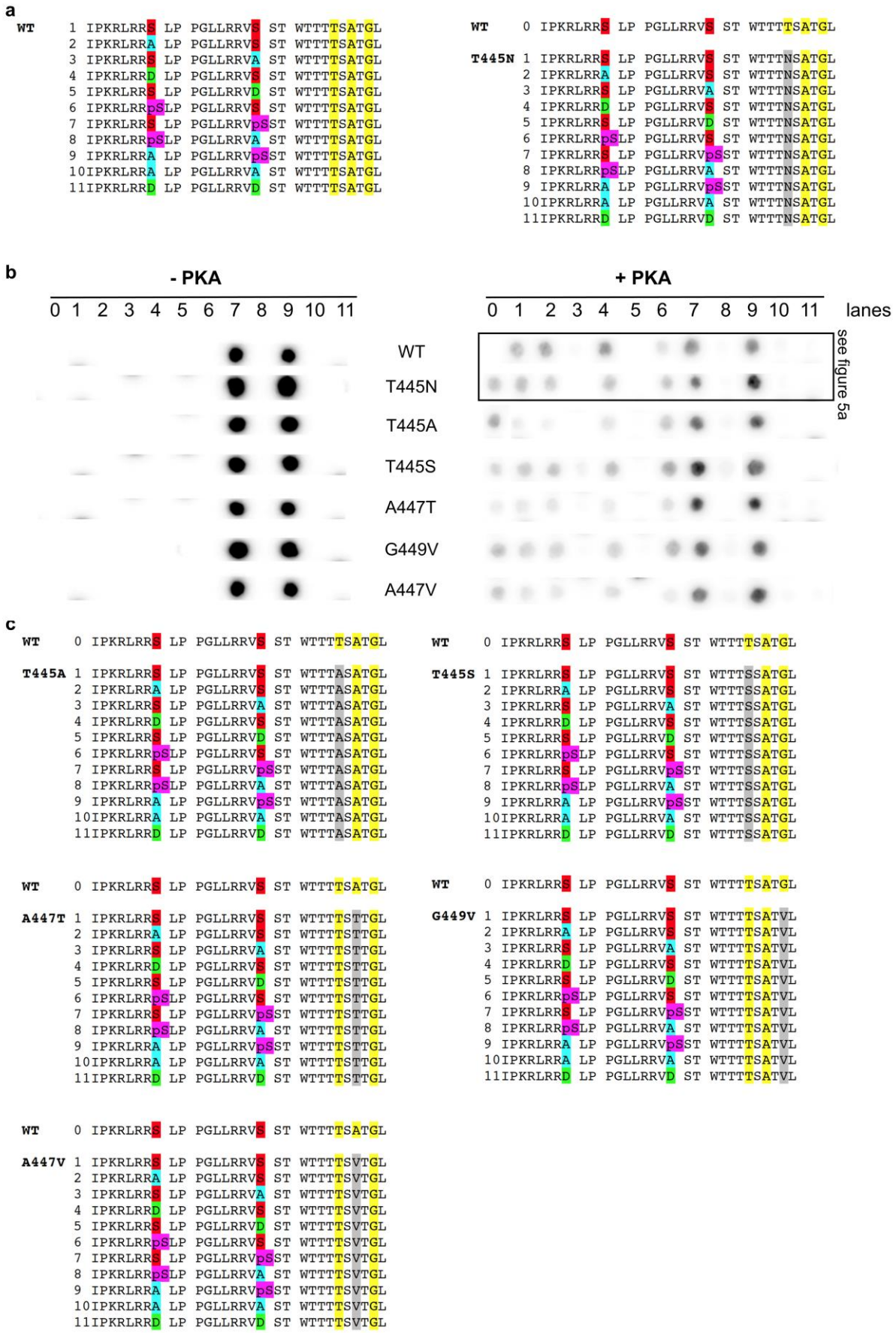

(a) Amino acid sequences of the synthesized peptide spots of figure 5a. Serines (S, red) at position 428 or 438 were replaced by alanine (A, blue) or asparagine (D, green) or pre-phosphorylated serine (pS, pink). The positions 445, 447 and 449 of the mutational amino acids are yellow, the mutational amino acid is marked in grey. **(b)** Phosphorylation of two peptide spot membranes (30-mers representing PDE3A isoleucine^{421}-leucine^{450}, see Figure 2a) without (- PKA) and with PKA (+PKA). Peptide spots of PDE3A WT and T445N (black frame) are the identical signals, shown in figure 5a. **(c)** Amino acid sequences of the synthesized peptide spots of supplementary figure 14b. The colour code is as indicated above. Serines at position 428 or 438 were replaced by alanine or asparagine or pre-phosphorylated serine. The positions 445, 447 and 449 of the mutational amino acids are yellow, each mutational amino acid is marked in grey.

Figure S14. Individual measurements of peptide spot quantifications and further peptide sequences.

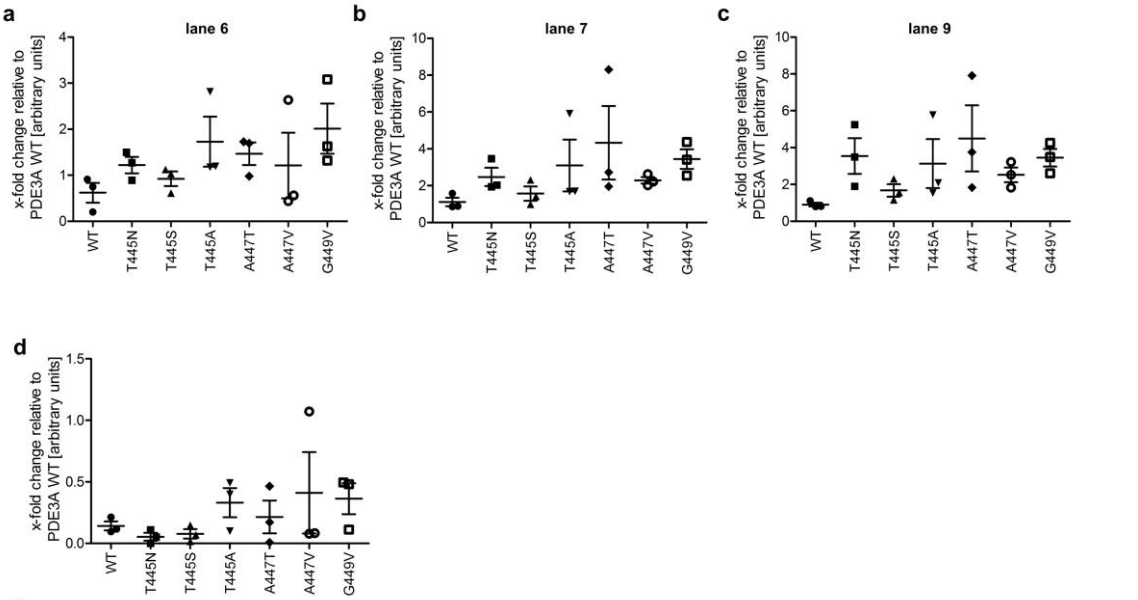

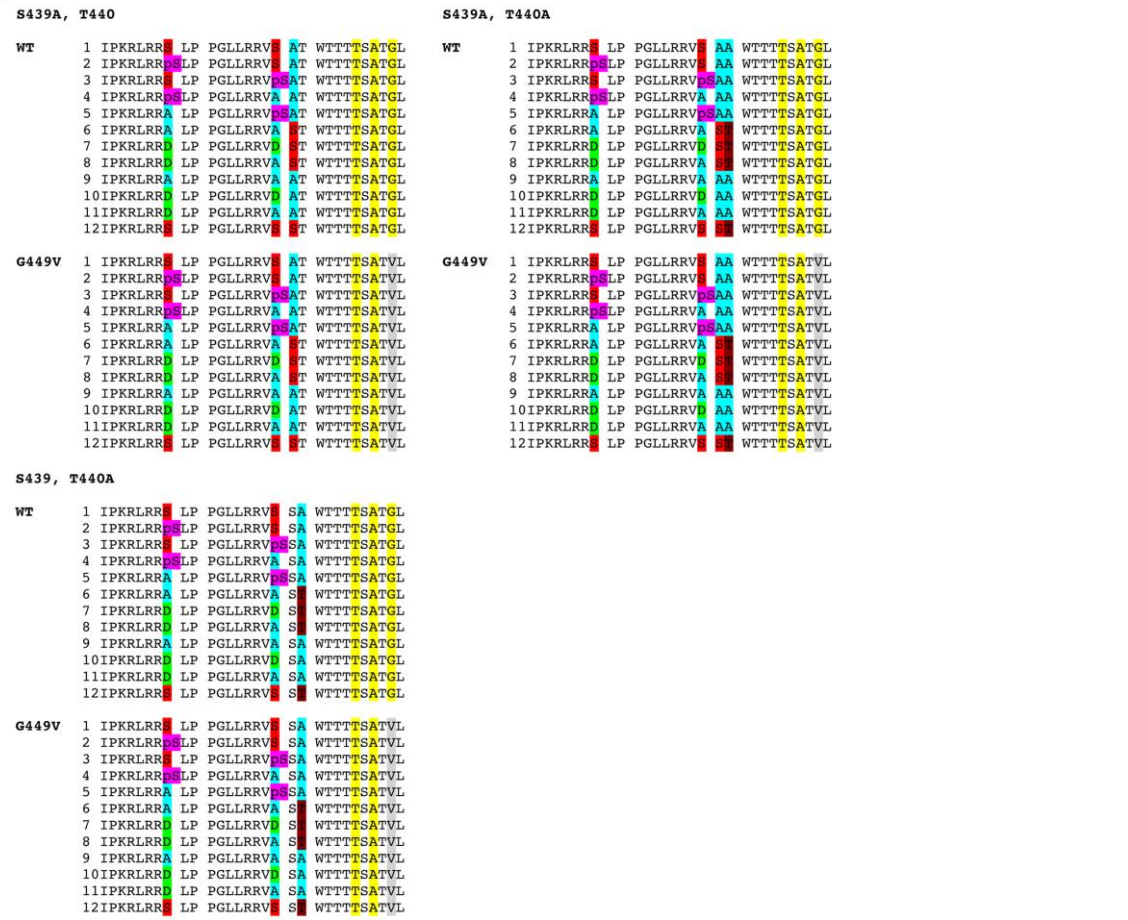

(a-c) Individual signal quantifications of peptide spots' experiments shown as pooled results in Figure 5b. The summarized data of all mutations from lane 6, 7 and 9 were statistically significant, determined by non-parametrical two-tailed Mann-Whitney rank sum testing (Figure 5b). **(d)** Signal quantifications of the six PDE3A mutational peptides and PDE3A wildtype (WT) of lane 3 from panel b (Ser^{428} and Ala^{438}) determined no significant changes after PKA phosphorylation, indicating that Ser^{428} is not differentially phosphorylated by PKA. **(e)** Peptide assay to further determine signal intensities at pre-phosphorylated Ser^{438} with alanine (A, blue) or asparagine (D, green) replacements or pre-phosphorylated serine (pS, pink) for the three different serines (S, red) at position 428, 438, or 439 and threonine (T, dark red) at position 440. **(f)** Amino acid sequences of the synthesized peptide spots of supplementary figure S14e. Serines at position 428 or 438 were replaced by alanine or asparagine or pre-phosphorylated serine. The colour code is as indicated above.

Figure S15. Michaelis-Menten kinetics of alanine substituted PDE3A1 and A2 wildtype and T445N.

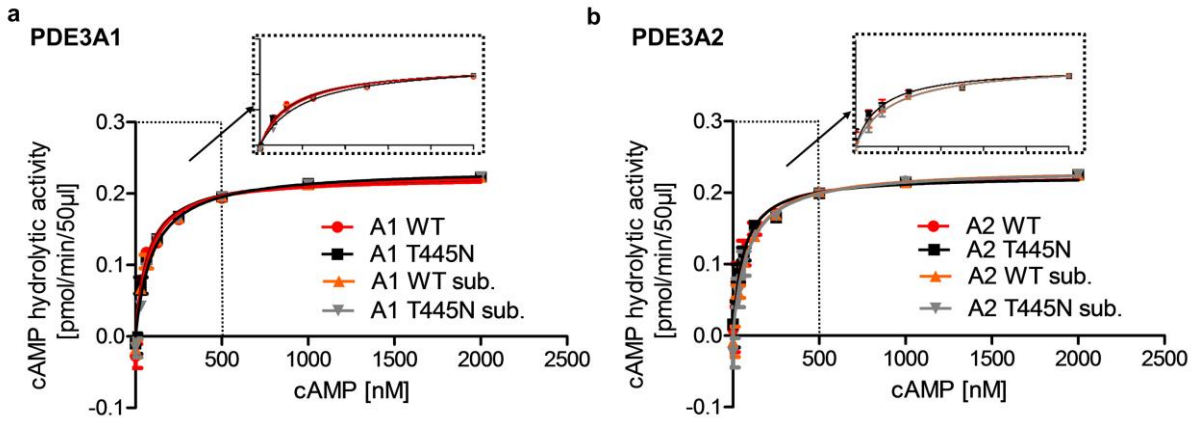

(a) Michaelis-Menten kinetics of FLAG-tagged PDE3A1 and **(b)** PDE3A2, comparing the phosphorylated wildtype (WT) and T445N enzymes with alanine substituted enzymes (sub.) at position 428, 438, 439 and 440. The prevented phosphorylation led to a decrease in the cAMP affinity. The values of the non-linear regression analysis were used to calculate the ratios of the hydrolytic activity shown in Figure 5c.

Methods.

Whole genome sequencing, Sanger sequencing and SNP analysis.

Complete Genomics performed whole genome sequencing of three affected patients and one control of a Turkish nuclear family.[17] Whole genomic DNA from EDTA-blood was extracted using standard procedures. A mean per-sample depth of coverage of 57.39x was reached. After bioinformatic analysis, data were further analyzed with CGA™-tools. Within the CG annotated coding genes' variations of the linkage interval, only the *PDE3A* missense mutation T445N was detected in three affected patients of the Turkish nuclear family. Numerous insertion, deletion or substitution events within the linkage region, indicating micro-mutations at the putative inversion breakpoints, were found. We selected heterozygous variations and excluded annotated SNPs, not detectable in the non-affected control, nor in the genome assembly hg19. They were further analyzed in a larger cohort (7 AFF and 7 NON, Supplementary Appendix Table S1). Sanger re-sequencing of seven affected patients and seven controls determined polymorphisms only. After the identification of the putative inversion-breakpoint regions by interphase FISH, the genomic regions with the CG sequencing reads were further analyzed in the CGI browser (data not shown). Reads for the genomic region of interest were extracted from CG annotated variations and visualized. None of the variations indicated the inversion breakpoints.

An Illumina HiSeq 2000 was used to generate 101-bp paired-end reads and 374 Gigabases of raw sequence data were mapped to the human reference GRCh37.3 with Novoalign yielding an average coverage of more than 100 fold. Single nucleotide variants and small indels were detected with the GATK toolkit,[18] annotated with ANNOVAR,[19] and analyzed on GeneTalk.[20] The structural variations were detected with BreakDancer,[21] and the previously reported inversion was additionally analyzed as described in Spielman et al., but did not reveal any inversion breakpoints.[22]

SNPs for haplotype construction or the *PDE3A* exon 4 to detect the mutations (fw: 5' aggatcacagtcttcaggaacc, rv: 5' agttgtgtcagcagattctgga), were PCR-amplified and sequenced using the Big Dye® Terminator Cycle Sequencing Kit v1.1 (Applied Biosystems). The analysis was performed on a 3130xl Genetic Analyzer (Applied Biosystems) using Gene Mapper® Software Version 4.0. SeqMan software (Lasergene Version 10.0; DNAStar) was used to evaluate the traces.

Whole mount RNA *in situ* hybridization.

In situ hybridizations were carried out using digoxygenin-UTP-labeled murine *Pde3a* sense and antisense riboprobes (coding sequence probe chr6: 141459712-141471161 bp, 3' UTR probe chr6:141498908-141499348, UCSC, mm10) according to standard protocols.

HeLa cells and chondrogenic induction of fibroblasts.

HeLa cells were ordered at ATCC, grown in DMEM, supplemented with 10 % FCS and 100 U/ml penicillin and 100 µg/ml streptomycin. The cells were frequently tested for mycoplasma contamination. Patients and controls-derived fibroblasts were cultured in Eagle's MEM 199 with 10% FCS, 100 U/ml penicillin and 100 µg/ml streptomycin. The chondrogenic induction of fibroblasts was done in pellet cultures with DMEM, supplemented with 10% FCS, 100 U/ml penicillin, and 100 µg/ml streptomycin, 1 x ITS-X (Life Technologies), 10 ng/ml hTGF-β1 (R&D Systems), 500 ng/ml rhIGF-1 (R&D Systems), 50 µM Lascorbic-2-phosphate (Sigma) and L-glutamine (PAA), for 21–28 days. Fibroblasts were fixed for 10 min with 4% paraformaldehyde (Sigma), were stained in 1% Alcian blue (Chroma, 3% acetic acid) for 30 min or 6% Safranin O (Sigma, dH_2O) for 2 min. Prior to microscopic documentation the cells were washed twice with 90% ethanol.

Expression plasmids.

Each of the six *PDE3A* mutations were introduced in the wildtype full-length *PDE3A* cDNA (NM_000921) clone (Origene, SC300151) by *in vitro* mutagenesis according to manufacturer's protocol (QuickChange II XL Site-Directed Mutagenesis Kit, Ambion Technologies). The recommended PCR extension times were doubled to amplify the large plasmids. In transfected HeLa cells, the PDE3A1 translation started from amino acid 146, PDE3A2 translation was initiated from position 299 and PDE3A3 translation could be started from position 483, but was not expressed in transiently transfected HeLa cells. The T445N mutation was also introduced into the FLAG-tagged *PDE3A1* and *PDE3A2* expression plasmids that we had previously characterized.[23] Recombinant *PDE3A1* and *PDE3A2* FLAG-tagged constructs and their substituted versions with alanine at positions 428, 438, 439 and 440 were used in Michaelis-Menten kinetics and IC_{50} measurements. Sanger sequencing validated the integrity of the entire *PDE3A* open reading frame of each plasmid.

cAMP and cGMP enzyme immuno-assay.

$4.5x10^5$ HeLa cells (ATCC) were seeded in 6 cm petri dish. After overnight incubation, cells were transfected with 1 pmol of each full-length *PDE3A* expression plasmid and 20 µl Fugene Xtreme Gene HP (Roche) for 48 h. Prior to cell lysis, 20 µM forskolin (Sigma) or 10 µM L-arginine (Sigma) stimulation was carried out for 30 min. The cell lysates were used for cAMP and cGMP assays (R&D Systems) that were performed according to the user's manual. BCA-quantified total protein of cell lysates served for normalization.

CFSE proliferation assay.

$4x10^5$ HeLa cells or $2x10^5$ VSMC, cultured in 20 % FCS, were labeled with carboxyfluorescein diacetate, succinimidyl ester (CFSE; 10 µM per $1x10^6$ cells) for each time point according to the manufacturer's recommendation (Life Technologies). CFSE-labelled cells were seeded 12-24 h prior to transfection with 500 fmol of each expression plasmid and 8 µl Fugene Xtreme Gene HP (Roche). Timepoint 0 h of CFSE-labelled cells was determined after overnight incubation and before transfection. Every 24 h post transfection, cells were analyzed in a BD FACSCalibur flow cytometer. Cell numbers were determined by normalizing PDE3A wildtype (WT, NM_000921) and the six PDE3A mutations to endogenous PDE3A of empty-vector-control-transfected HeLa cells. Differentiation of VSMC (see below) was performed for 14-21 days. VSMC differentiation media was changed after CFSE labelling to DMEM, supplemented with 20 % FCS and 1 ng/ml TGF-β1. Proliferation of VSMC was normalized to start point at 0 h.

PDE3A1-WT, PDE3A1-T445N FLAG-tag immuno-precipitation, Michaelis-Menten kinetics and IC_{50} measurements.

$2x10^6$ transfected HeLa cells transiently expressing FLAG-tagged versions of PDE3A1 or PDE3A2 were scraped from two 10 cm cell culture dishes in 1 ml of PBS. Prior to harvest, 20 µM forskolin (Sigma) or DMSO for controls were used to stimulate for 30 min. Short centrifugation (5 min, 4 °C, 1200 rpm) pelleted cells for lysis in 100 µl of RIPA buffer (50 mM Tris pH 7.8, 10 % Glycerol, 150 mM NaCl, 1 % Triton-X, 0.025 % sodium deoxycholate, 1 mM EDTA) supplemented with protease and phosphatase inhibitors (Complete and PhosSTOP, Roche Diagnostics). Cells were incubated for 10 min on ice and subsequently centrifuged (15 min, 4 °C, 14000 rpm, Eppendorf). ANTI-FLAG ® M2 Magnetic Beads (Sigma-Aldrich) were thoroughly resuspended. 80 µl beads for each lysate

were washed five times in Tris buffered saline, mixed thoroughly and placed on a magnetic separator to remove washing buffer. Equilibrated beads were loaded with equal amounts of protein lysate (BCA quantification) and incubated overnight at 4 °C on a rotating device. After discarding the supernatant, the beads were washed three times with Tris buffered saline supplemented with protease and phosphatase inhibitors. Washed beads bound to FLAG-PDE3A1-WT or FLAG-PDE3A1-T445N, respectively, were resuspended in 800 µl incubation buffer (10 mM Tris pH 8.0, 10 mM $MgCl_2$), 10 % were used for each cAMP hydrolysis assay. Incubation of purified beads-bound enzymes with cAMP in increasing concentrations or with the inhibitors milrinone or cGMP were done at 30 °C, 1100 rpm for 30 min. In the inhibitor assays another incubation at 30 °C, 1100 rpm for 30 min followed after the addition of 250 nM cAMP as substrate. Tubes were placed in a magnetic separator and supernatant was transferred in new tubes filled with neutralization buffer (cAMP Direct Immuno Assay Kit, Biovision). Further steps were performed as described in the instruction manual. Magnetic beads were resuspended in 10x SDS loading buffer (50 mM Tris pH 6.8, 1.6 % SDS, 4 % glycerol 0.6 % β-mercaptoethanol, bromophenolblue) and incubated for 5 min at 95 °C. Western blotting of each sample was used to validate equal enzyme loads for each condition. FLAG-PDE3A-WT and FLAG-PDE3A-T445N were detected using PDE3A (Bethyl Laboratories Inc.) and anti-PDE3A phospho Ser^{438} (S442B; University of Dundee) antibodies. Signals were visualized using Immobilon™ Western (Merck Millipore) and the Odyssey ® Fc Dual Mode Imaging System (Li-cor ®). K_M and IC_{50} values were calculated using the GraphPad Prism software (version 5.01). In contrast to the inaccurate linear-regression, we used the non-linear regression analysis with OLS (ordinary least squares) curve fitting and a Hill slope of -1 or 1, respectively, to determine the IC_{50} values or Michaelis-Menten (MM) kinetics shown in Figure 3 and 5 (Supplement Fig. 4, 5, 15). According to the GraphPad tutorials, the calculated MM-values were transformed to generate the double-reciprocal Lineweaver-Burke plots.

Mesenchymal stromal cell (MSC) extraction, cultivation, characterization and differentiation.

MSCs of the two affected patients and two non-affected related controls were extracted from peripheral blood in heparin sulfate.[24] We determined a frequency of 6% for successful MSC extractions from peripheral blood. Since the two controls were too old, their MSCs did not show the multilineage potential. The used and documented MSC controls were extracted from lipoaspirates of non-affected and non-related family members. The fat biopsies were washed with PBS/1% AntiAnti (Life Technologies). Larger tissue was mechanically destructed using a scalpel, the suspension was washed with PBS/1% AntiAnti over a 100 µm cell strainer. Consequent PBS washing removed erythrocytes and blood. The homogenization was done by collagenase I digest (0.1% in PBS) with 1 % BSA for 60 min at 37°C. After 10 min incubation with 15 ml DMEM (low glucose), the adipocytes on the surface were removed. The remaining cell suspension was filtered again using a 100 µm cell strainer and centrifuged for 10 min at room temperature at 1300 rpm. After discarding the supernatant, the cell pellet was washed with 15 ml DMEM and centrifuged again for 5 min. After centrifugation, the cells were resuspended in DMEM (low glucose), supplemented with 100 U/ml penicillin, 100 µg/ml streptomycin, 2 IU/ml heparin sulfate, 5% human fresh frozen plasma (FFP) and 5% concentrated thrombocytes. Dependent on the lipoaspirate's volume, the following dishes were used: 1 ml in 25 cm^2, up to 3 ml in 75 cm^2, more than 3 ml in 150 cm^2. After 24 hours, the cells were washed five times with PBS, then new media was added. After 3-4 days, stretched out, fibroblast-like cells were observed. Splitting ratio for sub-confluent MSCs was 1:5 or 1:6. Passages until P8 were used in the described experiments. Upon FACS characterization for $CD105^+$, $CD90^+$, $CD73^+$, $HLA\text{-}ABC^+$, $CD31^-$, $CD34^-$, $CD45^-$ and $HLA\text{-}DR^-$ cells, MSCs were differentiated. The adipogenic differentiation medium was DMEM (1 g/l glucose), 1 IU/ml heparin sulfate, 1% concentrated thrombocytes, 5% FFP, 100 U/ml penicillin, 100 µg/ml streptomycin, 1 µM dexamethasone, 100 µM L-ascorbic-2-phosphate,

60 µM indometacin and 0,5 µM IBMX and 10 µM insulin (Sigma). After 2-5 weeks of differentiation, cells were fixed with steams of 40% formalin for 10 minutes, washed twice with distilled water and stained for 3 minutes in 1% oil red. The differentiation time was dependent on the presence of fatty vacuoles. The osteogenic differentiation was performed within two weeks. The differentiation medium for the first week contained DMEM (1 g/l glucose), 1 IU/ml heparin sulfate, 1% concentrated thrombocytes, 5% FFP, 100 U/ml penicillin, 100 µg/ml streptomycin, 10 nM dexamethasone and 100 µM L-ascorbic-2-phosphate. The 2nd week, 100 ng/ml rhBMP2 (R&D Systems) and 10 mM β-glycerophosphate were added. After a PBS wash, cells were fixed with ice-cold methanol, air dried and stained in 0.5% alizarin red for 30 seconds. After a 15 minutes PBS wash, the calcium precipitates were microscopically photo-documented. The chondrogenic differentiation was performed in micromass pellet cultures for up to three weeks. DMEM (4.5 g/l glucose) was supplemented with 1 IU/ml heparin sulfate, 5% FFP, 1 x ITS-X (Life Technologies), 100 U/ml penicillin, 100 µg/ml streptomycin, 100 nM dexamethasone, 50 µM L-ascorbic-2-phosphate, 100 ng/µl rhIGF1, 10 ng/ml rhTGF-β1 (R&D Systems) and 1 mM sodium pyruvate. Chondrogenic pellets were fixed overnight with 4% PFA and paraffin embedded tissue was sectioned for toluidin blue staining. The smooth muscle differentiation medium was DMEM (1 g/l glucose), 1 IU/ml heparin sulfate, 5% FFP, 100 U/ml penicillin, 100 µg/ml streptomycin and 1 ng/ml rhTGF-β1. The medium was exchanged every two days for a period of 21 days.

FACS.

FACS staining of extracellular surface markers was done according to standard procedures in a BD FACSCalibur. The following antibodies were used: anti-CD105 (MHCD10504, Invitrogen), anti-CD90 (555595, BD Biosciences), anti-CD73 (550257, BD Biosciences),

anti-HLA-ABC (555552, BD Biosciences), anti-CD31 (555445, BD Biosciences), anti-CD34 (555821, BD Biosciences), anti-CD45 (555482, BD Biosciences), and anti-HLA-DR (555561, BD Biosciences).

Antibodies and Western blotting.

After 48 hours of transfection, HeLa cells were stimulated either with 20 µM forskolin (Sigma) or 100 ng/ml PMA for 30 min. Western blotting was performed according to standard protocols with 20 µg of total protein quantified in BCA test (ThermoScientific). Anti-PDE3A phospho Ser^{428} (S446B) and Ser^{438} (S442B) were ordered from the University of Dundee. Carol MacKintosh validated the antibodies' specificity and usage in several projects.[25,26] The following antibodies were also used: anti-PDE3A (A302-740A, Bethyl Laboratories Inc.), anti-PTHLH (ab41438, Abcam), anti-PTHLH (ab115488, Abcam), anti-β tubulin (sc-9104, Santa Cruz Biotechnology), anti-VASP phospho Ser^{157} (ab47268, Abcam), anti-VASP (sc-13975, Santa Cruz Biotechnology), anti-SMAα (ab8211, Abcam), anti-calponin (ab700, Abcam), anti-SM22α (ab10135, Abcam) and anti-Renilla luciferase (MAB4400, Millipore). The competitors for antibodies recognizing phosphorylated proteins, were the appropriate peptides from Santa Cruz and the University of Dundee. The detection of Renilla luciferase, co-transfected in HeLa transfections, indicated equal transfection and expression conditions. Blot signals were determined by HRP-mediated chemiluminescence (SuperSignal West Pico, ThermoScientific) and visualized in a PeqLab, Chemi-Smart 5000.

Immunofluorescence.

For semi-quantitative confocal microscopy to investigate proteins and their phosphorylation states, MSC, VSMC or transiently transfected HeLa cells were grown on glass coverslips. After one PBS-wash, the cells were fixed with fresh 4% paraformaldehyde for 10 min at RT

and permeabilized with 80 % methanol for 20 min at -20 °C. After blocking with 2% BSA/PBS and primary antibody incubation at appropriate dilution (see antibodies listed in section western blotting), staining was accomplished with Alexa-488 coupled secondary antibodies. Visualization was done with a BioRad MRC1024 attached to a Nikon Diaphot inverted microscope using the 488 nm line from an argon/krypton laser with a kalman filter of 3. After detection, the used pseudo-colors indicated expression levels from black (low) to red (high).

Luciferase reporter assays.

$5x10^4$ HeLa cells were seeded 12–24 h prior to transfection. Equal molarities were transiently transfected to compensate the diverse plasmid sizes. 75 fmol each of the CRE-luciferase construct (pGL4.29, Promega) and the full-length wildtype *PDE3A* or full-length mutation constructs were transfected with Fugene Extreme Gene HP (Roche), according to the manufacturer's recommendations. The CRE-luciferase construct harbored a cAMP responsive element that drove the luciferase transcription. Thus, the measured luciferase activity was dependent on the cellular cAMP level. 12.5 ng of pRL-TK (Promega) were added to control transfection efficiency. After 48 h of transfection, either total RNA was prepared or cell lysates were analyzed using the Dual-Glo Assay (Promega) in a Berthold luminometer. 4 h prior to cell lysis, forskolin, cilostazol or milrinone were added.[27] Forskolin activates adenylate cyclase for cAMP production. Enhanced forskolin-mediated cAMP levels, caused luciferase upregulation. L-Arginine enhances guanylate cyclase for cGMP production and was added for 10-15 min before cell lysis.[28] Since cGMP inhibits the PDE-mediated cAMP hydrolysis in a competitive manner, the luciferase transcription was upregulated. BAY 41-8543 also stimulates the soluble guanylate cyclase.[29] The media of transfected HeLa cells was supplemented with BAY 41-8543 (kindly provided by Dr. Damian Brockschnieder, Bayer AG), 30 min before harvesting. The compound (0.5 mg/ml) was solved in dimethyl

formamide (DMF):PBS (pH 7.2), 1:1. In all functional *in vitro* experiments, DMSO or DMF served as controls.

Peptide arrays, PKA phosphorylation of spot-synthesized peptides, and immunoblotting.

Peptide spots were generated by automatic SPOT synthesis using the Intavis ResPep-SL (Intavis) device as described previously.[30-33] Fmoc-protected amino acids were purchased from Intavis; phosphoserine (Fmoc-Ser(PO-(OBzl)OH)-OH) was from Novabiochem (Merck Millipore). Derivatized cellulose-membranes (amino-modified acid-stable cellulose membrane with PEG-spacer) were also purchased from Intavis.

The membranes were briefly soaked in ethanol, blocked in blocking buffer (5 % milk in TBS-T: Tris-HCl, 10 mM; NaCl, 150 mM; Tween 20, 0.05 %; pH 7.4) for 3 h at room temperature, and are subsequently washed twice with incubation buffer (Tris-HCl, 50 mM; $MgCl_2$, 5 mM; ATP, 100 µM). For phosphorylation of the peptides by PKA, His-tagged recombinant catalytic subunits (vector pET46) were purified from E. coli (strain Rosetta D3) as described for RIIα subunits.[34] The peptide spots were incubated with the recombinant catalytic subunits (1 nM) in incubation buffer for 1 h at 30°C. The membranes were washed three times with TBS-T. Phosphorylated Ser was detected with PKA phosphosubstrate antibody recognizing the consensus site RRX p(S/T) (Cell Signaling Technology) in blocking buffer overnight at 4°C.[35] The membranes were washed three times with TBS-T. Thereafter, horseradish peroxidase (HRP)-coupled donkey anti-rabbit secondary antibody (#711-036-153; Jackson Immuno Research) was added (3 h, RT), the membranes were washed three times with TBS-T, and an ECL reaction was carried out using Immobilon™ Western substrate (Merck Millipore). Signals were visualized with the Odyssey FC device (Li-Cor ®).

Pyrosequencing.

Pyrosequencing was done according to standard procedures. After cDNA synthesis of total RNA, the following oligonucleotides were used (fw: 5' biotin-ACC TCC CTG CCC TGT ATA, rv: 5' TTT GGT GAG GGT CAT CAT C, sequencing primer: 5' TAG ACC TGT GGC CGA).

TaqMan expression analysis.

RNA was prepared using Trizol® Reagent (Life Technologies) and reverse transcribed with the first strand cDNA synthesis kit (Fermentas). qRT-PCR was performed according to standard protocols on ABI 7500. TaqMan^{R} gene expression assays were used for *PTHLH* and *GAPDH* amplification (Life Technologies). Expression was quantified applying the ΔΔCt method.

Statistics.

The differentiation in smooth muscle cells and the functional *in vitro* experiments were reproduced 2-6 times. Numbers (n) of experiments are mentioned in the figure legends. Significance was determined by non-parametrical Wilcoxon-Mann-Whitney rank sum testing (*** $p<0.001$, ** $p<0.01$, * $p<0.05$). Scatter-plots show mean and T-bars indicate SEM (standard error of mean).

References.

1. Bilginturan, N., Zileli, S., Karacadag, S. & Pirnar, T. Hereditary brachydactyly associated with hypertension. *J Med Genet* **10**, 253-9 (1973).
2. Schuster, H. *et al.* Autosomal dominant hypertension and brachydactyly in a Turkish kindred resembles essential hypertension. *Hypertension* **28**, 1085-92 (1996).
3. Schuster, H. *et al.* A cross-over medication trial for patients with autosomal-dominant hypertension with brachydactyly. *Kidney Int* **53**, 167-72 (1998).
4. Naraghi, R. *et al.* Neurovascular compression at the ventrolateral medulla in autosomal dominant hypertension and brachydactyly. *Stroke* **28**, 1749-54 (1997).
5. Tank, J. *et al.* Autonomic nervous system function in patients with monogenic hypertension and brachydactyly: a field study in north-eastern Turkey. *J Hum Hypertens* **15**, 787-92 (2001).
6. Jordan, J. *et al.* Severely impaired baroreflex-buffering in patients with monogenic hypertension and neurovascular contact. *Circulation* **102**, 2611-8 (2000).
7. Bahring, S. *et al.* Autosomal-dominant hypertension with type E brachydactyly is caused by rearrangement on the short arm of chromosome 12. *Hypertension* **43**, 471-6 (2004).
8. Toka, O. *et al.* Childhood hypertension in autosomal-dominant hypertension with brachydactyly. *Hypertension* **56**, 988-94 (2010).
9. Pereda, A. *et al.* Brachydactyly E: isolated or as a feature of a syndrome. *Orphanet J Rare Dis* **8**, 141 (2013).
10. Toka, H.R. *et al.* Families with autosomal dominant brachydactyly type E, short stature, and severe hypertension. *Ann Intern Med* **129**, 204-8 (1998).
11. Lam, H.Y. *et al.* Performance comparison of whole-genome sequencing platforms. *Nat Biotechnol* **30**, 78-82 (2012).

12. Mills, R.E. *et al.* Mapping copy number variation by population-scale genome sequencing. *Nature* **470**, 59-65 (2011).

13. Dominici, M. *et al.* Minimal criteria for defining multipotent mesenchymal stromal cells. The International Society for Cellular Therapy position statement. *Cytotherapy* **8**, 315-7 (2006).

14. Gong, Z. & Niklason, L.E. Small-diameter human vessel wall engineered from bone marrow-derived mesenchymal stem cells (hMSCs). *Faseb J* **22**, 1635-48 (2008).

15. Chen, S., Evans, H.G. & Evans, D.R. FAM129B/MINERVA, a novel adherens junction-associated protein, suppresses apoptosis in HeLa cells. *J Biol Chem* **286**, 10201-9 (2011).

16. Song, G.J., Fiaschi-Taesch, N. & Bisello, A. Endogenous parathyroid hormone-related protein regulates the expression of PTH type 1 receptor and proliferation of vascular smooth muscle cells. *Mol Endocrinol* **23**, 1681-90 (2009).

17. Drmanac, R. *et al.* Human genome sequencing using unchained base reads on self-assembling DNA nanoarrays. *Science* **327**, 78-81 (2010).

18. McKenna, A. *et al.* The Genome Analysis Toolkit: a MapReduce framework for analyzing next-generation DNA sequencing data. *Genome Res* **20**, 1297-303 (2010).

19. Wang, K., Li, M. & Hakonarson, H. ANNOVAR: functional annotation of genetic variants from high-throughput sequencing data. *Nucleic Acids Res* **38**, e164 (2010).

20. Kamphans, T. & Krawitz, P.M. GeneTalk: an expert exchange platform for assessing rare sequence variants in personal genomes. *Bioinformatics* **28**, 2515-6 (2012).

21. Chen, K. *et al.* BreakDancer: an algorithm for high-resolution mapping of genomic structural variation. *Nat Methods* **6**, 677-81 (2009).

22. Spielmann, M. *et al.* Homeotic arm-to-leg transformation associated with genomic rearrangements at the PITX1 locus. *Am J Hum Genet* **91**, 629-35 (2012).

23. Vandeput, F. *et al.* Selective regulation of cyclic nucleotide phosphodiesterase PDE3A isoforms. *Proc Natl Acad Sci U S A* **110**, 19778-83 (2013).

24. Hofmann, N.A., Reinisch, A. & Strunk, D. Isolation and large scale expansion of adult human endothelial colony forming progenitor cells. *J Vis Exp* (2009).

25. Pozuelo Rubio, M., Campbell, D.G., Morrice, N.A. & Mackintosh, C. Phosphodiesterase 3A binds to 14-3-3 proteins in response to PMA-induced phosphorylation of Ser428. *Biochem J* **392**, 163-72 (2005).

26. Hunter, R.W., Mackintosh, C. & Hers, I. Protein kinase C-mediated phosphorylation and activation of PDE3A regulate cAMP levels in human platelets. *J Biol Chem* **284**, 12339-48 (2009).

27. Linglart, A. *et al.* Recurrent PRKAR1A mutation in acrodysostosis with hormone resistance. *N Engl J Med* **364**, 2218-26 (2011).

28. Knowles, R.G., Palacios, M., Palmer, R.M. & Moncada, S. Formation of nitric oxide from L-arginine in the central nervous system: a transduction mechanism for stimulation of the soluble guanylate cyclase. *Proc Natl Acad Sci U S A* **86**, 5159-62 (1989).

29. Stasch, J.P. *et al.* Pharmacological actions of a novel NO-independent guanylyl cyclase stimulator, BAY 41-8543: in vitro studies. *Br J Pharmacol* **135**, 333-43 (2002).

30. Hundsrucker, C. *et al.* High-affinity AKAP7delta-protein kinase A interaction yields novel protein kinase A-anchoring disruptor peptides. *Biochem J* **396**, 297-306 (2006).

31. Hundsrucker, C. *et al.* Glycogen synthase kinase 3beta interaction protein functions as an A-kinase anchoring protein. *J Biol Chem* **285**, 5507-21 (2010).

32. Coin, I., Beyermann, M. & Bienert, M. Solid-phase peptide synthesis: from standard procedures to the synthesis of difficult sequences. *Nat Protoc* **2**, 3247-56 (2007).

33. Stefan, E. *et al.* Compartmentalization of cAMP-dependent signaling by phosphodiesterase-4D is involved in the regulation of vasopressin-mediated water reabsorption in renal principal cells. *J Am Soc Nephrol* **18**, 199-212 (2007).

34. Schafer, G. *et al.* Highly functionalized terpyridines as competitive inhibitors of AKAP-PKA interactions. *Angew Chem Int Ed Engl* **52**, 12187-91 (2013).

35. Christian, F. *et al.* Small molecule AKAP-protein kinase A (PKA) interaction disruptors that activate PKA interfere with compartmentalized cAMP signaling in cardiac myocytes. *The Journal of biological chemistry* **286**, 9079-96 (2011).